P4.6

SIMULATIONS OF THE TURBULENCE AND DISPERSION PROCESSES IN A COASTAL REGION

Danijel Belušic[a]*, Darko Koracin[b], Igor Kos[c], Amela Jericevic[d] and Kristian Horvath[d]

[a] University of Zagreb, Zagreb, Croatia
[b] Desert Research Institute, Reno, Nevada
[c] Croatia Control Ltd., Zagreb, Croatia
[d] Meteorological and Hydrological Service, Zagreb, Croatia

1 INTRODUCTION

So far there have been no advanced air-pollution studies using state-of-the-art dispersion models over the Northern Adriatic coastal region. Several active industrial emission sources such as oil refineries and thermal powerplants are located there, especially near the city of Rijeka. This is a complex terrain area with abrupt changes between the sea and high steep mountains. It is thus necessary to investigate the influence of the pollutants on air quality in that region with a model capable of capturing flow complexity related to the structure of the terrain. Hence, we employed a recently developed Lagrangian particle dispersion model ALPS (Atmospheric Lagrangian Particle Stochastic model) to study the dispersion processes under different meteorological conditions that are characteristic for the area.

2 LAGRANGIAN PARTICLE MODEL

The model basic concepts are as follows (e.g. Koracin *et al.*, 1998, 1999): predefined number of particles is released at each prescribed time step and the calculation of their trajectories is performed. The trajectories are determined according to:

$$
\begin{aligned}
x(t+\Delta t) &= x(t) + u(t)\Delta t \\
y(t+\Delta t) &= y(t) + v(t)\Delta t \\
z(t+\Delta t) &= z(t) + w(t)\Delta t
\end{aligned}
\qquad (1)
$$

where t is time, x, y and z are the position of the particle and u, v and w are wind velocities composed of the corresponding predicted mean wind components $\overline{u}$, $\overline{v}$ and $\overline{w}$, and subgrid-scale velocities u_r, v_r and w_r:

$$
\begin{aligned}
u(t) &= \overline{u}(t) + u_r(t) \\
v(t) &= \overline{v}(t) + v_r(t) \\
w(t) &= \overline{w}(t) + w_r(t)
\end{aligned}
$$

Mean wind velocity components are obtained from a mesoscale meteorological model while subgrid-scale velocities are determined as:

$$
\begin{aligned}
u_r(t) &= u_r(t-\Delta t)R_u(\Delta t) + u_s(t-\Delta t) \\
v_r(t) &= v_r(t-\Delta t)R_v(\Delta t) + v_s(t-\Delta t) \\
w_r(t) &= w_r(t-\Delta t)R_w(\Delta t) + w_s(t-\Delta t)
\end{aligned}
\qquad (2)
$$

where R_u, R_v and R_w, are corresponding Lagrangian autocorrelation functions and u_s, v_s and w_s are the stochastic fluctuations.

The Lagrangian autocorrelation functions are given by:

$$
\begin{aligned}
R_u(\Delta t) &= e^{-\Delta t / T_{Lu}} \\
R_v(\Delta t) &= e^{-\Delta t / T_{Lv}} \\
R_w(\Delta t) &= e^{-\Delta t / T_{Lw}}
\end{aligned}
\qquad (3)
$$

where T_{Lu}, T_{Lv} and T_{Lw} are the Lagrangian time scales for the three wind components which are determined from the following relations:

$$
\begin{aligned}
T_{Lu} &\propto h / \sqrt{(\overline{u'u'})} \\
T_{Lv} &\propto h / \sqrt{(\overline{v'v'})} \\
T_{Lw} &\propto h / \sqrt{(\overline{w'w'})}
\end{aligned}
\qquad (4)
$$

where $(\overline{u'u'})$, $(\overline{v'v'})$ and $(\overline{w'w'})$ are the maximal variances in the domain obtained from the meteorological model as a fraction of the predicted turbulent kinetic energy (TKE), and h represents scale height dependant on the stability of the atmosphere.

3 METEOROLOGICAL SIMULATIONS

3.1 Meteorological model

We employed the nonhydrostatic mesoscale numerical model for unsaturated air using a higher order turbulence closure (MEMO6). It solves prognostic equations for momentum, potential temperature, TKE and specific humidity. The calculated TKE is used for turbulence parameterization in ALPS. More detailed description of the model and its performance can be found in previous publications (e.g. Moussiopoulos, 1995; Caballero and Lavagnini, 2002; Klaic and Nitis, 2002; Klaic *et al.*, 2003a).

* *Corresponding author address:* Danijel Belušic, Geophysical Institute, Faculty of Science, University of Zagreb, Horvatovac bb, 10000 Zagreb, Croatia

3.2 Sea breeze case

Sea breeze was simulated from 18–19 June 2000 on a 300 x 300 km^2 domain at the horizontal resolution of 3 km and time step of 10 s. The center of the domain was placed at 45°N, 15°E (see Fig. 1). The model top was set at 8 km above the surface. In the vertical, 30 layers were selected with a finer resolution at lower altitudes. The initial and boundary conditions were obtained from the Udine (46.03°N, 13.18°E, 94 m ASL) radiosonde data. The soundings were available every 6 h (00, 06, 12 and 18 UTC each day), except at 06 UTC on 19 June.

The emission source in the ALPS model was located at Rijeka (45.33°N, 14.45°E, 120 m ASL), at 100 m height. It is the height of refinery stack near Rijeka, but can also be taken as a reference height for other sources in the Rijeka area.

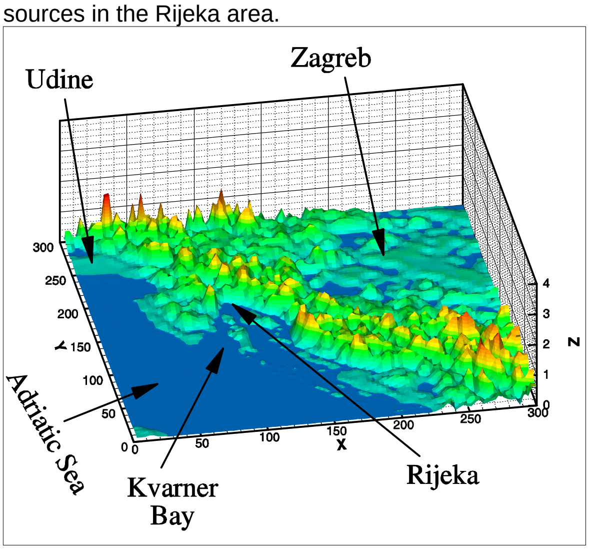

Figure 1. Modeling domain viewed from the southwest with topography contours plotted every 100 m.

3.3 Bora case

The simulation was performed from 13–15 January 2002. The modeling domain was the same as for the sea breeze case, except that the model top was set at 10 km above the surface. The model was driven by the Zagreb–Maksimir (45.82°N, 16.03°E, 128 m ASL) radiosonde data, which were available every 12 h (00 and 12 UTC each day).

The Lagrangian model setup was the same in both cases.

4 RESULTS

4.1 Sea breeze case

First few hours of the simulation (Fig. 2) were characterized by predominantly southerly winds advecting the plume northward, which then spreads through mountain gaps. The air was stable and thus the plume remained confined within the first few hundred meters.

Sea breeze started approximately 12 hours after the beginning of the simulation (around 12 UTC on 18 June). Figure 3 shows the plume position at 17 UTC on 18 June, when the sea breeze lasted for about 5 h. Although the part of the plume located near the ground is advected towards the land, the upper part is moving in opposite direction (i.e., towards the sea).

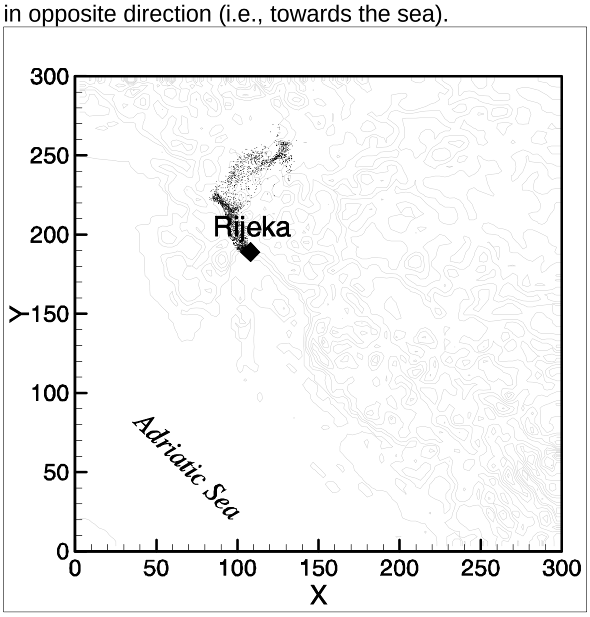

Figure 2. Top view of the dispersion during the sea breeze case at 05 UTC on 18 June – beginning of the simulation.

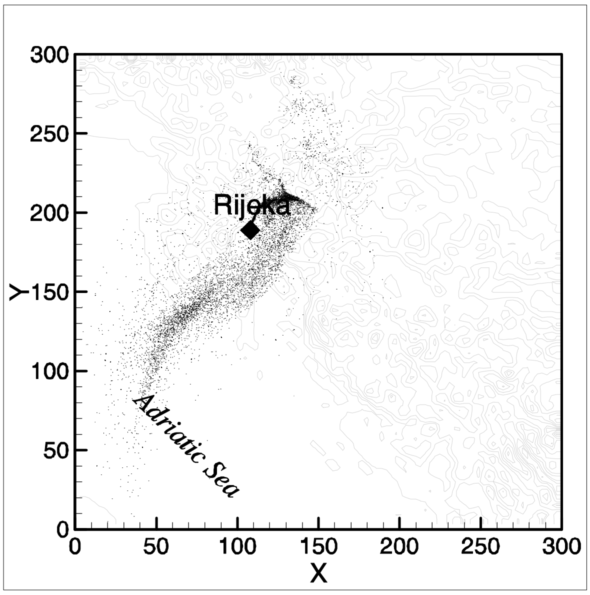

Figure 3. Same as Fig. 2, except for 17 UTC on 18 June – sea breeze with a strong vertical shear of the wind direction.

This can be attributed to three combined effects: 1) the boundary layer being statically very unstable and its top reaching over 1 km, 2) related to the instability, the air moving towards northeast (i.e., towards the land) impinges upon high mountains and is lifted upwards due to high vertical velocities generated by the obstacle and additionally enhanced by the unstable atmospheric conditions, and 3) starting at about 900 m above the ground the wind changes direction to northeast and its speed increases, hence advecting the uplifted plume (which reached the heights above 1 km) back towards the sea. The last effect is of synoptic origin and is thus not a part of the standard sea breeze conditions.

The situation at 05 UTC next day is shown in Fig. 4. The land breeze started to develop around 00 UTC on 19 June. At that time a small cyclonic meso-vortex, approximately 20 km in diameter, appeared in Kvarner Bay just south of Rijeka. During the next few hours it was slowly advected towards southwest and grew to around 40 km in diameter. Approximately 6 h later it disappeared. The plume rotor-like formation in Fig. 4 was thus generated by that vortex. We believe that the vortex originates from wind shear generated by the complexities in topography, where the northern part of the vortex, due to pronounced mountain gaps, had stronger northeasterly winds than the southern part. The rest of the plume, which is dispersed at higher altitudes, is the residue from previous hours transported and dispersed by the sea breeze.

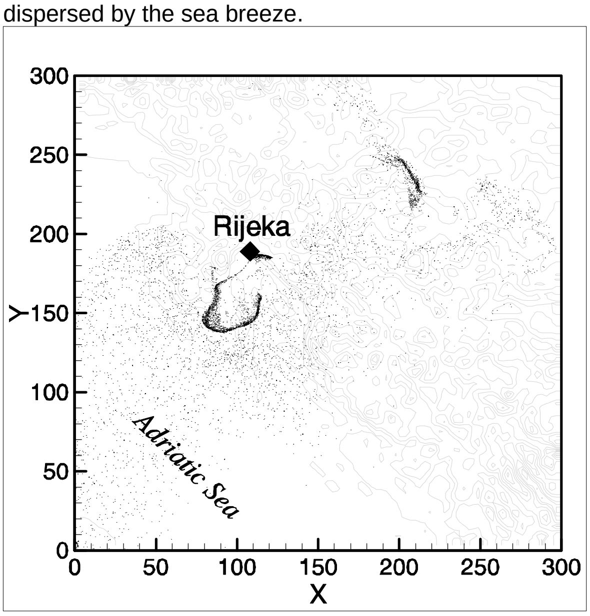

Figure 4. Same as Fig. 2, except for 05 UTC on 19 June – the land breeze, associated meso-vortex and the plume inland that remained from the sea breeze.

Finally, the development of the sea breeze on 19 June began around 12 UTC. Figure 5 shows the position of the plume at 17 UTC. As in the previous day, the instability forced part of the plume to propagate vertically, but this time the winds had predominantly southwesterly directions up to 3 km above the ground and thus the plume is positioned inland.

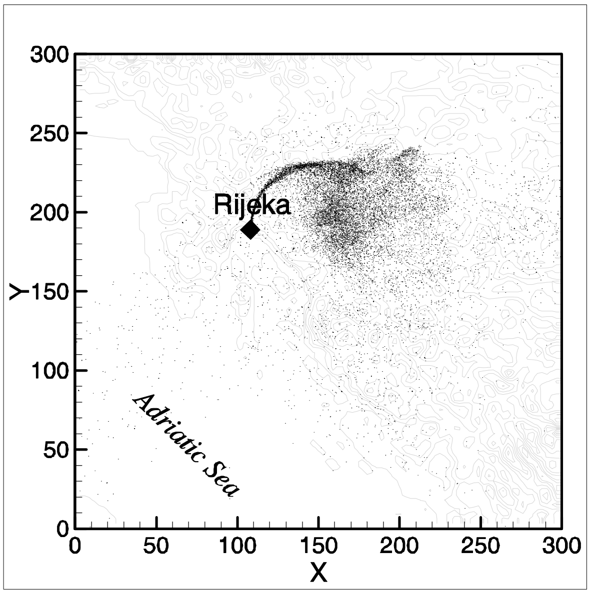

Figure 5. Same as Fig. 2, except for 17 UTC on 19 June – a developed sea breeze stage.

4.2 Bora case

During the first 12 h of the simulation the wind directions were dominantly northwesterly and thus there was no bora flow. Figure 6 shows the plume position 10 h after the start of the simulation. Due to northwesterly winds, the plume spread horizontally along the coast towards southeast. As the atmosphere was statically stable, there were only minor vertical displacements. One can thus observe spreading and splitting of the plume through mountain gaps, and also the appearance of rotor-like features after passing a gap.

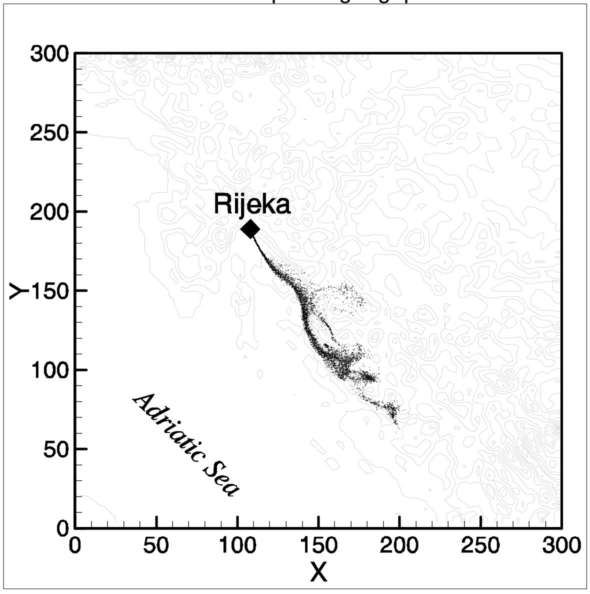

Figure 6. Top view of the dispersion during the bora case at 10 UTC on 13 January – prior to bora onset.

The wind direction started to turn to northeasterly around 13 UTC on 13 January and the bora began approximately 4 h later. Thus, Fig. 7 shows the plume position 5 h after the bora onset. A part of the plume spread vertically, but most of it remained near the surface in the first 200 m. The surface part of the plume reveals horizontal structures that resemble vorticity filaments (Klaic *et al.*, 2003b) or potential vorticity banners (Grubišic, 2000; 2004) previously observed and simulated over the eastern Adriatic coast. They were here induced by the alongshore horizontal variability of the magnitudes of the bora wind speed, i.e., the appearance of local minima and maxima related to variations in the topography. Nevertheless, there is a general tendency of the plume movement towards west/southwest, i.e., to the open sea. This is a first indication that the bora will act as a mechanism that improves air quality in this region.

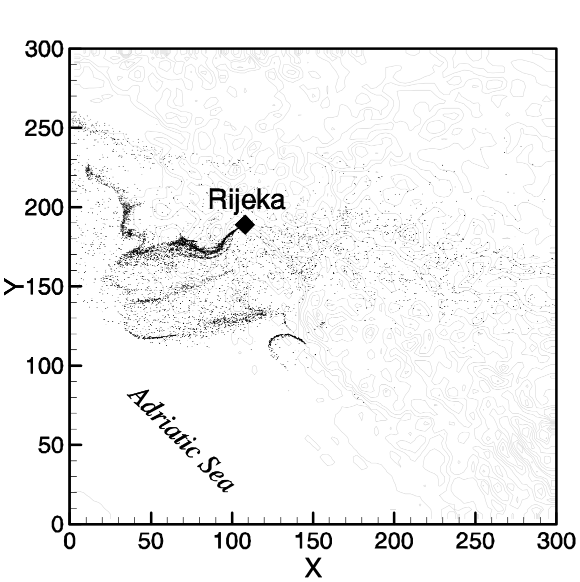

Figure 7. Same as Fig. 6, except for 22 UTC on 13 January – the beginning stage of the bora.

Finally, Fig. 8 shows developed stage of the bora, 17 h after the onset. The maximal wind speeds in the domain reached 20 m/s (18 m/s at Rijeka). At that time, plume is completely advected towards the open sea, and there are no traces of the pollutants over the land. At even later times, only a narrow trail extending from Rijeka to southeast remained (not shown).

The turbulence structures of the two studied cases are quite different. The sea breeze case is characterized by a pronounced temporal variation, where the TKE has maximum values during the daytime (reaching over 3 $m^2\ s^{-2}$) and almost disappears during the night. Contrary to that, there is no noticeable daily variation in the bora case, but two distinct TKE maxima appear in the vertical, the first being near the ground and the second at about 500 m. Its values reach over 5 $m^2\ s^{-2}$.

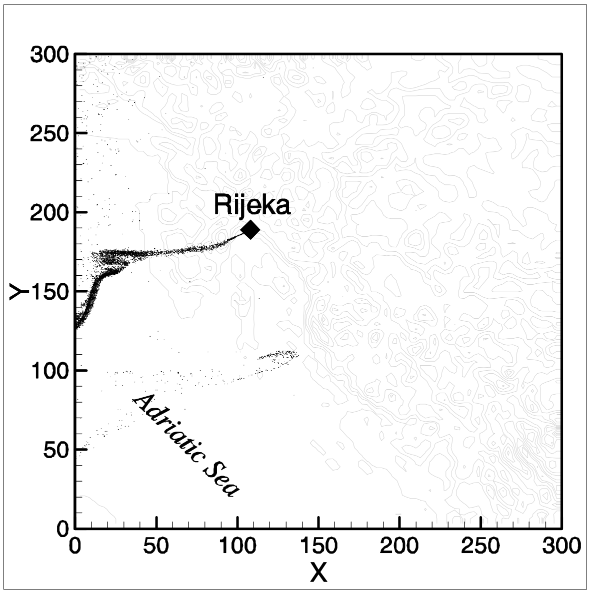

Figure 8. Same as Fig. 6, except for 10 UTC on 14 January – the developed bora.

5 SUMMARY AND CONCLUSIONS

We performed numerical simulations of the dispersion and turbulence processes in the Adriatic coastal region under two diverse but frequent meteorological situations using the meteorological model MEMO6 and the Lagrangian particle dispersion model ALPS. The complexity of the terrain, including the irregular land-sea border and high steep mountains with many gaps and passes, induced very intricate inhomogeneous flow patterns which became visible in the ALPS model results.

An overall picture, obtained from the ALPS results, of the sea breeze and bora impact on air quality in the area, indicates the possibility of recirculation of the atmospheric pollutants during sea and land breeze, with particular emphasis on the sea breeze situation where the pollutants may travel far inland (over 100 km) in a few hours (5 h in the simulation), thus deteriorating air quality in that region. On the other hand, under the bora conditions the plume is being advected far to the open sea which then results in a significant improvement of air quality in the coastal area.

This study also confirms the necessity of performing air-quality studies over this complex area with the advanced dispersion models, whose input fields should be taken from high resolution meteorological models.

6 REFERENCES

Caballero, R. and Lavagnini, A., 2002: A numerical investigation of the sea breeze and slope flows around Rome. *Nouvo Cimento*, **25 C**, 287–304.

Grubišic, V., 2000: Bora driven PV banners over the Adriatic: Preliminary results. *MAP Newsletter* **13**, 66–67.

Grubišic, V., 2004: Bora driven potential vorticity banners over the Adriatic. *Q. J. R. Meteorol. Soc*., in press.

Klaic, Z. B. and Nitis, T., 2002: Application of mesoscale model (MEMO) to the greater Zagreb area during summertime anticyclonic weather conditions. *Geofizika*, **18-19**, 31–43.

Klaic, Z. B., Belušic, D., Bulic, I. H. and Hrust, L., 2003a: Mesoscale modeling of meteorological conditions in the lower troposphere during a winter stratospheric ozone intrusion over Zagreb, Croatia. *J. Geophys. Res.*, **108**, 4720.

Klaic, Z. B., Belušic, D., Grubišic, V., Gabela, L. and Coso, L., 2003b: Mesoscale airflow structure over the northern Croatian coast during MAP IOP 15 – a major Bora event. *Geofizika*, **20**, 23–61.

Koracin, D., Isakov, V. and Frye, J., 1998: A Lagrangian particle dispersion model (LAP) applied to transport and dispersion of chemical tracers in complex terrain. Preprints 10th Joint Conf. of the Appl. of Air Pollution Meteor. with the Air and Waste Manag. Assoc. (AWMA), AMS, Phoenix, AZ, 227–230.

Koracin, D., Isakov V., Podnar D. and Frye J., 1999: Application of a Lagrangian random particle dispersion model to the short-term impact of mobile emissions. Proceedings of the Transport and Air Pollution Conference, Graz, Austria, 31 May – 2 June 1999.

Moussiopoulos, N., 1995: The EUMAC Zooming model, a tool for local-to-regional air quality studies. *Meteorol. Atmos. Phys.*, **57**, 115–133.